crystallization is frequently conducted continuously in a vacuum evaporating draft-tube baffled crystallizer to produce crystalline particles, whereas the falling-film crystallizer is used for melt crystallization to produce a dense layer of crystals.

Drying

A number of factors influence the selection of a dryer from the many different types available. These factors are dominated by the nature of the feed, whether it be granular solids, a paste, a slab, a film, a slurry, or a liquid. Other factors include the need for agitation, the type of heat source (convection, radiation, conduction, or microwave heating), and the degree to which the material must be dried. The most commonly employed continuous dryers include tunnel, belt, band, turbo-tray, rotary, steam-tube rotary, screw-conveyor, fluidized-bed, spouted-bed, pneumatic-conveyor, spray, and drum dryers.

7.4 SEQUENCING OF ORDINARY DISTILLATION COLUMNS FOR THE SEPARATION OF NEARLY IDEAL FLUID MIXTURES

Multicomponent mixtures are often separated into more than two products. Although one piece of equipment of complex design might be devised to produce all the desired products, a sequence of two-product separators is more common.

For nearly ideal feeds, such as hydrocarbon mixtures and mixtures of a homologous series, for example, alcohols, the most economical sequence will often include only ordinary distillation columns provided that the following conditions hold:

1. The relative volatility between the two selected key components for the separation in each column is > 1.05.
2. The reboiler duty is not excessive. An example of an excessive duty occurs in the distillation of a mixture with a low relative volatility between the two key components, where the light key component is water, which has a very high heat of vaporization.
3. The tower pressure does not cause the mixture to approach its critical temperature.
4. The overhead vapor can be at least partially condensed at the column pressure to provide reflux without excessive refrigeration requirements.
5. The bottoms temperature at the tower pressure is not so high that chemical decomposition occurs.
6. Azeotropes do not prevent the desired separation.
7. Column pressure drop is tolerable, particularly if operation is under vacuum.

Column Pressure and Type of Condenser

During the development of distillation sequences, it is necessary to make at least preliminary estimates of column operating pressures and condenser types (total or partial). The estimates are facilitated by the use of the algorithm in Figure 7.9, which is conservative. Assume that cooling water is available at 90°F, sufficient to cool and condense a vapor to 120°F. The bubble-point pressure is calculated at 120°F for an estimated distillate composition. If the computed pressure is less than 215 psia, use a total condenser unless a vapor distillate is required in which case use a partial condenser. If the pressure is less than 30 psia, set the condenser pressure to 30 psia and avoid near-vacuum operation. If the distillate bubble-point pressure is greater than 215 psia, but less than 365 psia, use a partial condenser. If it is greater than 365 psia, determine the dew-point pressure for the distillate as a vapor. If the pressure is greater than 365 psia, operate the condenser at 415 psia with a suitable refrigerant in place of cooling water. For the selected condenser pressure, add 10 psia to estimate the bottoms pressure,

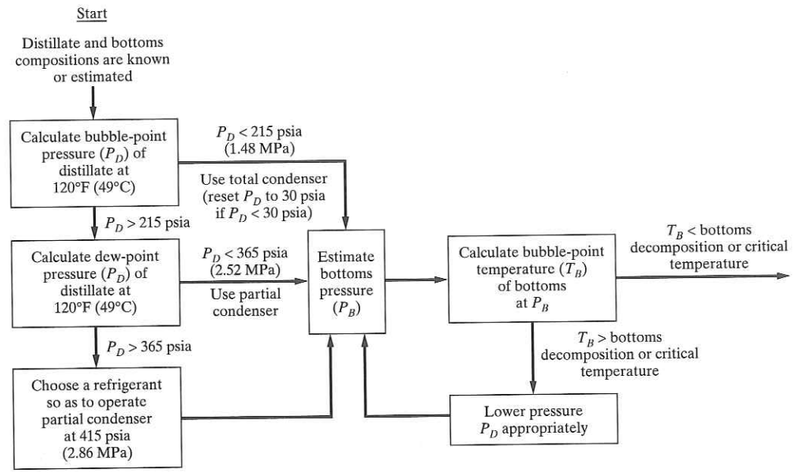

Figure 7.9 Algorithm for establishing distillation column pressure and condenser type.

and compute the bubble-point temperature for an estimated bottoms composition. If that temperature exceeds the decomposition or critical temperature of the bottoms, reduce the condenser pressure appropriately.

Number of Sequences of Ordinary Distillation Columns

Initial consideration is usually given to a sequence of ordinary distillation columns, where a single feed is sent to each column and the products from each column number just two, the distillate and the bottoms. For example, consider a mixture of benzene, toluene, and biphenyl. Because the normal boiling points of the three components (80.1, 110.8, and 254.9°C, respectively) are widely separated, the mixture can be conveniently separated into three nearly pure components by ordinary distillation. A common process for separating this mixture is the sequence of two ordinary distillation columns shown in Figure 7.10a. In the first column, the most volatile component, benzene, is taken overhead as a distillate final product. The bottoms is a mixture of toluene and biphenyl, which is sent to the second column for separation into the two other final products: a distillate of toluene and a bottoms of biphenyl, the least volatile component.

Even if a sequence of ordinary distillation columns is used, not all columns need give nearly pure products. For example, Figure 7.10b shows a distillation sequence for the separation of a mixture of ethylbenzene, *p*-xylene, *m*-xylene, and *o*-xylene into only three products: nearly pure ethylbenzene, a mixture of *p*- and *m*-xylene, and nearly pure *o*-xylene. The para and meta isomers are not separated because the normal boiling points of these two compounds differ by only 0.8°C, making separation by distillation impractical.

Note in Figure 7.10 that it takes a sequence of two ordinary distillation columns to separate a mixture into three products. Furthermore, other sequences can produce the same final products. For example, the separation of benzene, toluene, and biphenyl, shown in Figure 7.10a, can also be achieved by removing biphenyl as bottoms in the first column, followed by the separation of benzene and toluene in the second column. However, the separation of toluene from benzene and biphenyl by ordinary distillation in the first column is impossible,

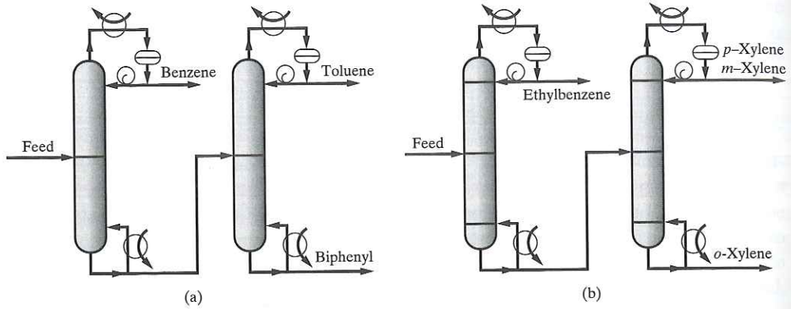

Figure 7.10 Distillation configurations for separation of ternary mixtures: (a) separation of a benzene-toluene-biphenyl mixture; (b) separation of xylene isomers.

because toluene is intermediate in volatility. Thus, the number of possible sequences is limited to two for this case of the separation of a ternary mixture into three nearly pure products.

Now consider the more general case of the synthesis of all possible ordinary distillation sequences for a multicomponent feed that is to be separated into P final products, which are nearly pure components and/or multicomponent mixtures. The components in the feed are ordered by volatility, with the first component being the most volatile. This order is almost always consistent with that for normal boiling point if the mixture forms nearly ideal liquid solutions, such that Eq. (7.3) applies. Assume that the order of volatility of the components does not change as the sequence proceeds. Furthermore, assume that any multicomponent products contain only components that are adjacent in volatility. For example, suppose that the previously cited mixture of benzene, toluene, and biphenyl is to be separated into toluene and a multicomponent product of benzene and biphenyl. With ordinary distillation, it would be necessary first to produce products of benzene, toluene, and biphenyl, and then blend the benzene and biphenyl.

An equation for the number of different sequences of ordinary distillation columns, N_s, to produce a number of products, P, can be developed in the following manner. For the first separator in the sequence, $P - 1$ separation points are possible. For example, if the desired products are A, B, C, D, and E in order of decreasing volatility, then the possible separation points are $5 - 1 = 4$, as follows: A–B, B–C, C–D, and D–E. Now let j be the number of final products that must be developed from the distillate of the first column. For example, if the separation point in the first column is C–D, then $j = 3$ (A, B, C). Then $P - j$ equals the number of final products that must be developed from the bottoms of the first column. If N_i is the number of different sequences for i final products, then, for a given separation point in the first column, the number of sequences is $N_j N_{P-j}$. But in the first separator, $P - 1$ different separation points are possible. Thus, the number of different sequences for P products is the following sum:

$$N_s = \sum_{j=1}^{P-1} N_j N_{P-j} = \frac{[2(P-1)]!}{P!(P-1)!} \tag{7.9}$$

Application of Eq. (7.9) gives results shown in Table 7.2 for sequences producing up to 10 products. As shown, the number of sequences grows rapidly as the number of final products increases.

Equation (7.9) gives five possible sequences of three columns for a four-component feed. These sequences are shown in Figure 7.11. The first, where all final products but one are distillates, is often referred to as the *direct sequence*, and is widely used in industry because

Table 7.2 Number of Possible Sequences for Separation by Ordinary Distillation

Number of Products, P	Number of Separators in the Sequence	Number of Different Sequences, N_s
2	1	1
3	2	2
4	3	5
5	4	14
6	5	42
7	6	132
8	7	429
9	8	1,430
10	9	4,862

distillate final products are more free of impurities such as objectionable high-boiling compounds and solids. If the purity of the final bottoms product (D) is critical, it may be produced as a distillate in an additional column called a *rerun* (or *finishing*) column. If all products except one are bottoms products, the sequence is referred to as the *indirect sequence*. This sequence is generally considered to be the least desirable sequence because of difficulties in achieving purity specifications for bottoms products. The other three sequences in Figure 7.11 produce two products as distillates and two products as bottoms. In all sequences except one, at least one final product is produced in each column.

EXAMPLE 7.1

Ordinary distillation is to be used to separate the ordered mixture C_2, $C_3^=$, C_3, $1\text{–}C_4^=$, nC_4 into the three products C_2; ($C_3^=$, $1\text{–}C_4^=$); (C_3, nC_4). Determine the number of possible sequences.

SOLUTION

Neither multicomponent product contains adjacent components in the ordered list. Therefore, the mixture must be completely separated with subsequent blending to produce the ($C_3^=$, $1\text{–}C_4^=$) and (C_3, nC_4) products. Thus, from Table 7.2 with P taken as 5, $N_s = 14$. ■

Heuristics for Determining Favorable Sequences

When the number of products is three or four, designing and costing all possible sequences can best determine the most economical sequence. Often, however, unless the feed mixture has a wide distribution of component concentrations or a wide variation of relative volatilities for the possible separation points, the costs will not vary much and the sequence selection may be based on operation factors. In that case, the direct sequence is often the choice. Otherwise, a number of heuristics that have appeared in the literature, starting in 1947, have proved useful for reducing the number of sequences for detailed examination. The most useful of these heuristics are:

1. Remove thermally unstable, corrosive, or chemically reactive components early in the sequence.
2. Remove final products one by one as distillates (the direct sequence).
3. Sequence separation points to remove, early in the sequence, those components of greatest molar percentage in the feed.
4. Sequence separation points in the order of decreasing relative volatility so that the most difficult splits are made in the absence of the other components.
5. Sequence separation points to leave last those separations that give the highest-purity products.
6. Sequence separation points that favor near equimolar amounts of distillate and bottoms in each column.

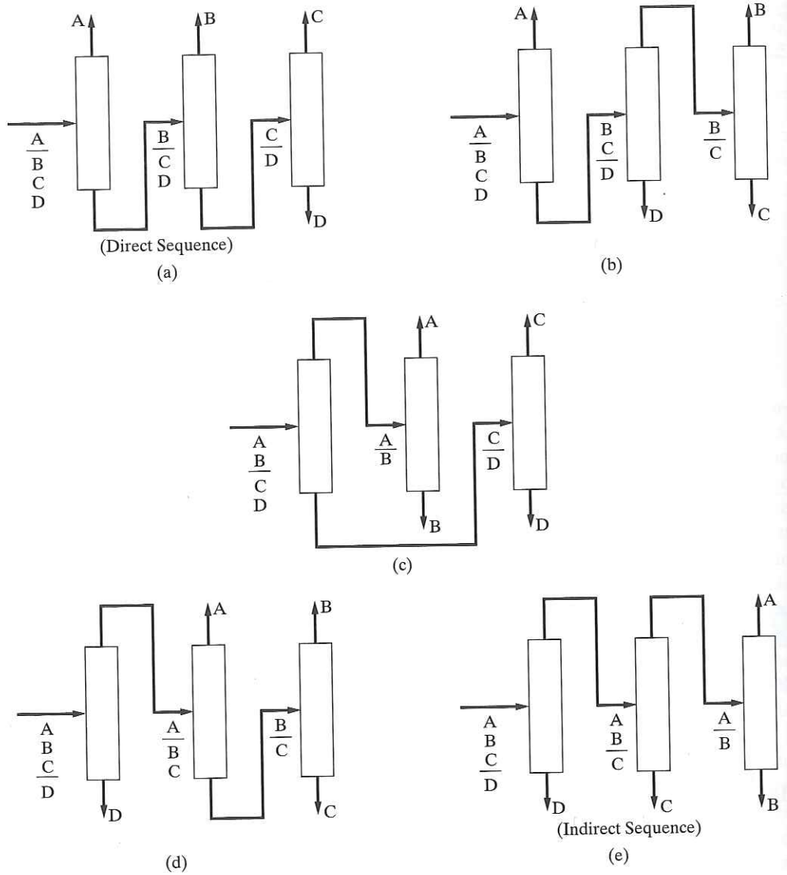

Figure 7.11 The five sequences for a four-component feed.

None of these heuristics require column design and costing. Unfortunately, however, these heuristics often conflict with each other. Thus, more than one sequence will be developed, and cost and other factors will need to be considered to develop an optimal final design. When energy costs are relatively high, the sixth heuristic often leads to the most economical sequence. Heuristics 2–6 are consistent with observations about the effect of the nonkey components on the separation of two key components. These nonkey components can increase the reflux and boilup requirements, which, in turn, increase column diameter and reboiler operating cost. These, and the number of trays, are the major factors affecting the investment and operating costs of a distillation operation.

EXAMPLE 7.2

Consider the separation problem shown in Figure 7.12a, except that separate isopentane and *n*-pentane products are also to be obtained with 98% recoveries. Use heuristics to determine a good sequence of ordinary distillation units.

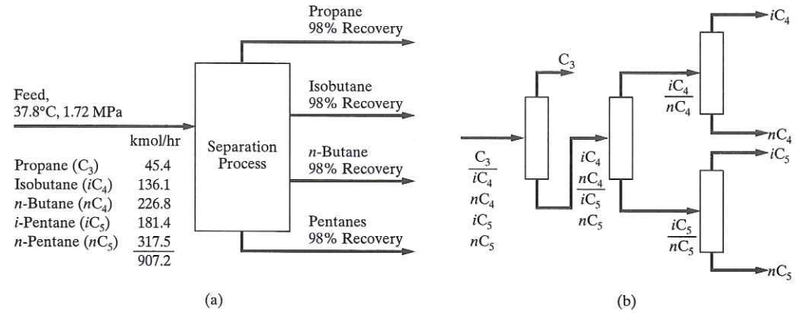

Figure 7.12 Synthesis problem and separation train for Example 7.2: (a) paraffin separation problem; (b) sequence developed from heuristics.

SOLUTION

Approximate relative volatilities for all adjacent pairs are

Component pair	Approximate α at 1 atm
C_3/iC_4	3.6
iC_4/nC_4	1.5
nC_4/iC_5	2.8
iC_5/nC_5	1.35

For this example, there are wide variations in both relative volatility and molar percentages in the process feed. The choice is Heuristic 4, which dominates over Heuristic 3 and leads to the sequence shown in Figure 7.12b, where the first split is between the pair with the highest relative volatility. This sequence also corresponds to the optimal arrangement. ■

Marginal Vapor Rate Method

When application of the above heuristics for sequencing ordinary distillation columns is uncertain or conflicting results are obtained, it is preferable to employ sequencing methods that rely on column design and, in some cases, cost estimation. Exhaustive search to calculate the annualized cost of every sequence can determine the optimal sequence, provided that column-operating conditions are optimized, and may be justified for sequences involving just three or possibly four products. However, less rigorous methods are available that can produce good, although not always optimal, sequences. These methods, which attempt to reduce the search space, include those of Hendry and Hughes (1972), Rodrigo and Seader (1975), Gomez and Seader (1976), Seader and Westerberg (1977), and the marginal vapor rate (MV) method of Modi and Westerberg (1992). The latter method outperforms the other methods and can be applied without the necessity of complete column designs and calculations of costs.

For a given split between two key components, Modi and Westerberg (1992) consider the difference in costs between the separation in the absence of nonkey components and the separation in the presence of nonkey components, defining this difference as the marginal annualized cost (MAC). They show that a good approximation of MAC is the MV, which is the corresponding difference in molar vapor rate passing up the column. The sequence with the minimum sum of column MVs is selected. The good approximation is due to the fact that vapor rate is a good measure of cost because it is a major factor in determining column diameter as well as reboiler and condenser areas (thus, column and heat exchanger capital costs) and reboiler and condenser duties (thus, heat exchanger annual operating costs).

A convenient method for determining the molar vapor rate in an ordinary distillation column separating a nearly ideal system uses the Underwood equations to calculate the minimum reflux ratio, R_{min}. This is readily accomplished, as in the example below, with a process simulation program. The design reflux ratio is taken as $R = 1.2\,R_{min}$. By material balance, the molar vapor rate, V, entering the condenser is given by $V = D(R + 1)$, where D is the molar distillate rate. Assuming that the feed to the column is a bubble-point liquid, the molar vapor rate through the column will be nearly constant at this value of V. In making the calculations of MV, the selection of product purities is not critical because the minimum reflux ratio is not sensitive to those purities. Thus, to simplify the material balance calculations, it is convenient to assume nearly perfect separations with the light and lighter-than-light key components leaving in the distillate and the heavy and heavier-than-heavy key components leaving in the bottoms. Column top and bottom pressures are estimated with Figure 7.9. The column feed pressure is taken as the average of the top and bottom pressures.

EXAMPLE 7.3

Use the marginal vapor rate (MV) method to determine a sequence for the separation of light hydrocarbons specified in Figure 7.12a, except: (1) remove the propane from the feed, (2) ignore the given temperature and pressure of the feed, and (3) strive for recoveries of 99.9% of the key components in each column. Use a process simulation program, with the Soave–Redlich–Kwong equation of state for K-values and enthalpies, to set top and bottom column pressures and estimate the reflux ratio with the Underwood equations.

SOLUTION

To produce four nearly pure products from the four-component feed, five sequences of three ordinary distillation columns each are shown in Figure 7.11. Let A = isobutane, B = n-butane, C = isopentane, and D = n-pentane. A total of 10 unique separations are embedded in Figure 7.11. These are listed in Table 7.3, together with the results of the calculations for the top column pressure, P_{top}, in kPa; the molar distillate rate, D, in kmol/hr; and the reflux ratio, R, using the shortcut (Fenske–Underwood–Gilliland or FUG) distillation model of the CHEMCAD process simulation program. This model applies the Underwood equations to estimate the minimum reflux ratio, as described by Seader and Henley (1998). Column feeds were computed as bubble-point liquids at P_{top} + 35 kPa. Also included in Table 7.3 are values of the column molar vapor rate, V, in kmol/hr and marginal vapor rate, MV, in kmol/hr.

From Table 7.3, the sum of the marginal vapor rates is calculated for each of the five sequences in Figure 7.11. The results are given in Table 7.4.

Table 7.4 shows that the preferred sequence is the one that performs the two most difficult separations, A/B and C/D, in the absence of nonkey components. These two separations are far more difficult than the separation, B/C. The direct sequence is the next best. ■

Table 7.3 Calculations of Marginal Vapor Rate, MV

Separation	Column Top Pressure (kPa)	Distillate Rate, D (kmol/hr)	Reflux Ratio ($R = 1.2\,R_{min}$)	Vapor Rate, $V = D(R + 1)$ (kmol/hr)	Marginal Vapor Rate (kmol/hr)
A/B	680	136.2	10.7	1,594	0
A/BC	680	136.2	11.9	1,757	163
A/BCD	680	136.2	13.2	1,934	340
B/C	490	226.8	2.06	694	0
AB/C	560	362.9	1.55	925	231
B/CD	490	226.8	3.06	921	227
AB/CD	560	362.9	2.11	1,129	435
C/D	210	181.5	13.5	2,632	0
BC/D	350	408.3	6.39	3,017	385
ABC/D	430	544.4	4.96	3,245	613

Table 7.4 Marginal Vapor Rates for the Five Possible Sequences

Sequence in Figure 7.11	Marginal Vapor Rate, MV (kmol/hr)
(a) Direct	567
(b)	725
(c)	435
(d)	776
(e) Indirect	844

Complex and Thermally Coupled Distillation Columns

Following the development of an optimal or near-optimal sequence of simple, two-product distillation columns, revised sequences involving complex, rather than simple, distillation columns should be considered. Some guidance is available from a study by Tedder and Rudd (1978a, b) of the separation of ternary mixtures (A, B, and C in order of decreasing volatility) in which eight alternative sequences of one to three columns were considered, seven of which are shown in Figure 7.13. The configurations include the direct and indirect sequences (I and II), two interlinked cases (III and IV), five cases that include the use of side streams (III, IV, V, VI, and VII), and one case (V) involving a column with two feeds. All columns in Cases I, II, V, VI, and VII have condensers and reboilers. In Cases III and IV, the first column has a condenser and reboiler. In Case III, the rectifier column has a condenser only, while the stripper in Case IV has a reboiler only. The interlinking streams that return from the second column to the first column thermally couple the columns in Cases III and IV.

As shown in Figure 7.14, optimal regions for the various configurations depend on the process feed composition and on an ease-of-separation index (ESI), which is defined as the relative volatility ratio, $\alpha_{A,B}/\alpha_{B,C}$. It is interesting to note that a ternary mixture is separated into three products with just one column in Cases VI and VII, but the reflux requirement is excessive unless the feed contains a large amount of B, the component of intermediate volatility, and little of the component that is removed from the same section of the column as B. Otherwise, if the feed is dominated by B but also contains appreciable amounts of A and C, the prefractionator case (V) is optimal. Perhaps the biggest surprise of the study is the superiority of distillation with a vapor sidestream rectifier, which is favored for a large region of the feed composition when ESI > 1.6. The results of Figure 7.14 can be extended to multicomponent separation problems involving more than three components, if difficult ternary separations are performed last.

Case V in Figure 7.13 consists of a prefractionator followed by a product column, from which all three final products are drawn. Each column is provided with its own condenser and reboiler. As shown in Figure 7.15, eliminating the condenser and reboiler in the prefractionator and providing, instead, reflux and boilup to that column from the product column can thermally couple this arrangement, which is referred to as a Petlyuk system after its chief developer and is described by Petlyuk et al. (1965). The prefractionator separates the ternary-mixture feed, ABC, into a top product containing A and B and a bottom product of B and C. Thus, component B is split between the top and bottom streams exiting from the prefractionator. The top product is sent to the upper section of the product column, while the bottom product is sent to the lower section. The upper section of the product column provides the reflux for the prefractionator, while the lower section provides the boilup. The product column separates its two feeds into a distillate of A, a sidestream of B, and a bottoms of C. Fidkowski and Krolikowski (1987) determined the minimum molar boilup vapor requirements for the Petlyuk system and the other two thermally coupled systems (III and IV) in Figure 7.13, assuming constant relative volatilities, constant molar overflow, and bubble-point liquid feed and products. They compared the requirements to those of the conventional direct and indirect sequences shown as Cases I and II in Figure 7.13 and proved

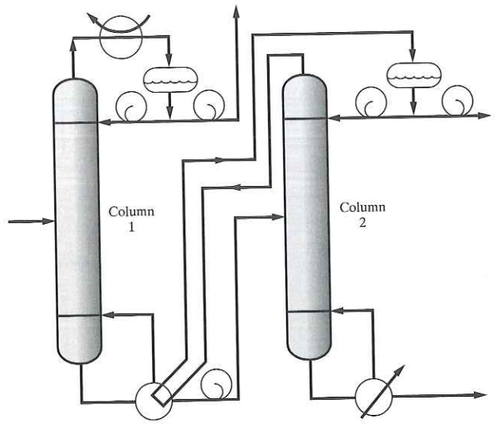

Figure 7.17 Heat-integrated direct sequence of two distillation columns.

components are not close-boiling because all of the reboiler heat must be supplied at the highest temperature and all of the condenser heat must be removed at the lowest temperature; and (2) the difficulty in controlling the fractions of vapor and liquid streams in the product column that are returned to the prefractionator as boilup and reflux, respectively. The Petlyuk system can be embodied into a single column, with a significantly reduced capital cost, by using a dividing-wall column (also called divided wall and column-in-column), a concept described in a patent by Wright (1949) and shown by his patent drawing in Figure 7.16. Because the dividing-wall column makes possible savings in both energy and capital, and because control difficulties appear to have been solved, it is attracting much attention. The first dividing-wall column was installed by BASF in 1985. A number of such columns using packing have been installed in the last 15 years and the first dividing-wall column using trays was recently announced. Agrawal and Fidkowski (1998) present other thermally fully coupled (FC) systems of distillation columns that retain the benefit of a minimum vapor requirement and afford easier control. Energy savings can also be achieved by heat-integrating the two columns in a direct sequence. In Figure 7.17, Column 2 is operated at a higher pressure than Column 1, such that the condenser duty of Column 2 can provide the reboiler duty of Column 1. Rev et al. (2001) show that heat-integrated systems are often superior in annualized cost to the Petlyuk system. For further discussion of heat-integrated distillation columns, see Sections 10.9, 20.1, and 21.3.

7.5 SEQUENCING OF OPERATIONS FOR THE SEPARATION OF NONIDEAL FLUID MIXTURES

When a multicomponent fluid mixture is nonideal, its separation by a sequence of ordinary distillation columns will not be technically and/or economically feasible if relative volatilities between key components drop below 1.05 and, particularly, if azeotropes are formed. For such mixtures, separation is most commonly achieved by sequences comprised of ordinary distillation columns, enhanced distillation columns, and/or liquid–liquid extraction equipment. Membrane and adsorption separations can also be incorporated into separation sequences, but their use is much less common. Enhanced distillation operations include extractive distillation, homogeneous azeotropic distillation, heterogeneous azeotropic distillation, pressure-swing distillation, and reactive distillation. These operations are considered in detail in *Perry's Chemical Engineers' Handbook* (Perry and Green, 1997) and by Seader and Henley (1998), Stichlmair and Fair (1998), and Doherty and Malone (2001). A design-oriented introduction to enhanced distillation is presented here.

In many processes involving oxygenated organic compounds, such as alcohols, ketones, ethers, and acids, often in the presence of water, distillation separations are complicated by the presence of azeotropes. Close-boiling mixtures of hydrocarbons (e.g., benzene and cyclohexane, whose normal boiling points only differ by 1.1°F) can also form azeotropes. For these and other mixtures, special attention must be given to the *distillation boundaries* in the composition space that confine the compositions for any one column to lie within a bounded region of the composition space. To introduce these boundaries, leading to approaches for the synthesis of separation trains, several concepts concerning azeotropes and *residue curves* and *distillation lines* are reviewed in the subsections that follow.

Azeotropy

Azeotrope is an ancient Greek word that is translated "to boil unchanged," meaning that the vapor emitted has the same composition as the liquid (Swietoslawski, 1963). When classifying the many azeotropic mixtures, it is helpful to examine their deviations from Raoult's law (Lecat, 1918).

When two or more fluid phases are in physical equilibrium, the chemical potential, fugacity, or activity of each species is the same in each phase. Thus, in terms of species mixture fugacities for a vapor phase in physical equilibrium with a single liquid phase,

$$\bar{f}_j^V = \bar{f}_j^L \qquad j = 1, \ldots, C \tag{7.10}$$

Substituting expressions for the mixture fugacities in terms of mole fractions, activity coefficients, and fugacity coefficients,

$$y_j \bar{\phi}_j^V P = x_j \gamma_j^L f_j^L \qquad j = 1, \ldots, C \tag{7.11}$$

where $\bar{\phi}$ is a mixture fugacity coefficient, γ is a mixture activity coefficient, and f is a pure-species fugacity.

For a binary mixture with an ideal liquid solution ($\gamma_j^L = 1$) and a vapor phase that forms an ideal gas solution and obeys the ideal gas law ($\bar{\phi}_j^V = 1$ and $f_j^L = P_j^s$), Eq. (7.11) reduces to the following two equations for the two components 1 and 2:

$$y_1 P = x_1 P_1^s \tag{7.12a}$$
$$y_2 P = x_2 P_2^s \tag{7.12b}$$

where P_j^s is the vapor pressure of species j.

Adding Eqs. (7.12a and 7.12b), noting that mole fractions must sum to one,

$$(y_1 + y_2)\, P = P = x_1 P_1^s + x_2 P_2^s = x_1 P_1^s + (1 - x_1)\, P_2^s = P_2^s + (P_1^s - P_2^s) x_1 \tag{7.13}$$

This linear relationship between the total pressure, P, and the mole fraction, x_1, of the most volatile species is a characteristic of Raoult's law, as shown in Figure 7.18a for the benzene-toluene mixture at 90°C. Note that the bubble-point curve (P–x) is linear between the vapor pressures of the pure species (at $x_1 = 0, 1$), and the dew-point curve (P–y_1) lies below it. When the (x_1, y_1) points are graphed at different pressures, the familiar vapor–liquid equilibrium curve is obtained, as shown in Figure 7.18b. Using McCabe–Thiele analysis, it is shown readily that for any feed composition, there are no limitations to the values of the mole fractions of the distillate and bottoms products from a distillation tower.

However, when the mixture forms a nonideal liquid phase and exhibits a positive deviation from Raoult's law ($\gamma_j^L > 1, j = 1, 2$), Eq. (7.13) becomes

$$P = x_1 \gamma_1^L P_1^s + (1 - x_1)\, \gamma_2^L P_2^s \tag{7.14}$$

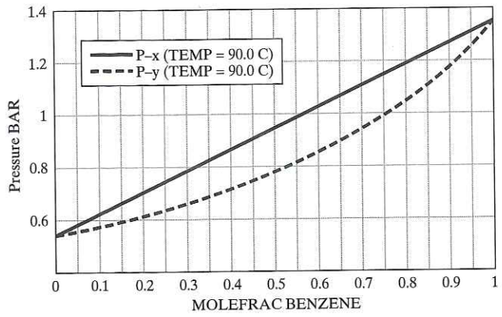

(a)

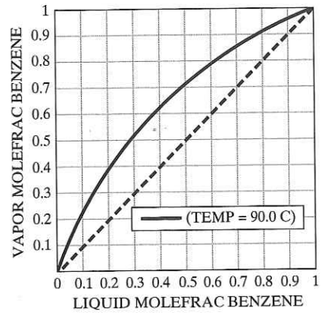

(b)

Figure 7.18 Phase diagrams for the benzene–toluene mixture at 90°C, calculated using ASPEN PLUS: (a) *P–x–y* diagram: (b) *x–y* diagram.

Furthermore, if the boiling points of the two components are close enough, the bubble- and dew-point curves may reach a maximum at the same composition, which by definition is the azeotropic point. Such a situation is illustrated in Figure 7.19a for the isopropyl ether (1)–isopropyl alcohol (2) binary at 70°C. Figure 7.19b shows the corresponding *x–y* diagram, and Figure 7.19c shows the bubble- and dew-point curves on a *T–x–y* diagram at 101 kPa. Note the *minimum-boiling azeotrope* at 66°C, where $x_1 = y_1 = 0.76$. Feed streams having lower isopropyl ether mole fractions cannot be purified beyond 0.76 in a distillation column, and streams having higher isopropyl ether mole fractions have distillate mole fractions that have a lower bound of 0.76. Consequently, the azeotropic composition is commonly referred to as a *distillation boundary*.

Similarly, when the mixture exhibits the less-common negative deviation from Raoult's law ($\gamma_j^L < 1, j = 1, 2$), both the bubble- and dew-point curves drop below the straight line that represents the bubble points for an ideal mixture, as anticipated by examination of Eq. (7.14). Furthermore, when the bubble- and dew-point curves have the same minimum, an azeotropic composition is defined, as shown in Figure 7.20a for the acetone–chloroform binary at 64.5°C, where $x_1 = y_1 = 0.35$. For this system, Figures 7.20b and 7.20c show the corresponding *x–y* diagram and *T–x–y* diagram at 101 kPa. On the latter diagram, the azeotropic point is at a maximum temperature, and consequently, the system is said to have a *maximum-boiling azeotrope*. In this case, feed streams having lower acetone mole fractions cannot be purified beyond 0.35 in the bottoms product of a distillation column, and streams having

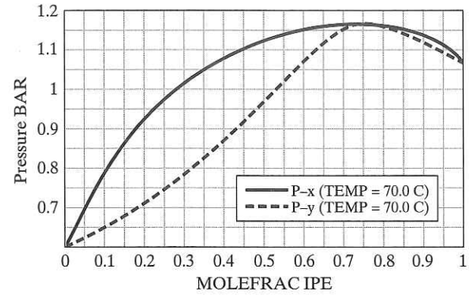

(a)

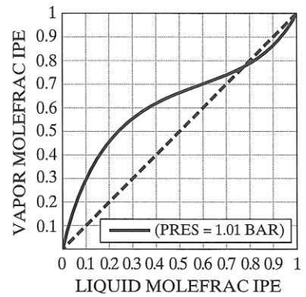

(b)

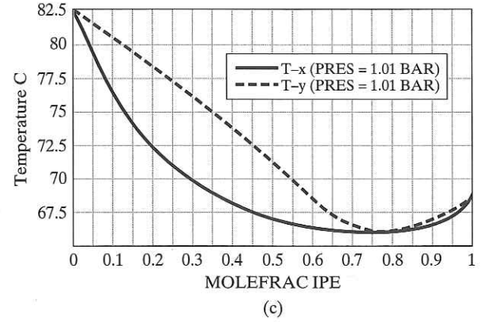

(c)

Figure 7.19 Phase diagrams for the isopropyl ether–isopropyl alcohol binary computed using ASPEN PLUS: (a) *P–x–y* diagram at 70°C; (b) *x–y* diagram at 101 kPa; (c) *T–x–y* diagram at 101 kPa.

higher acetone mole fractions have a lower bound of 0.35 in the acetone mole fraction of the bottoms product.

In summary, at a homogeneous azeotrope, $x_j = y_j$, $j = 1, \ldots, C$, the expression for the equilibrium constant, K_j for species j becomes unity. Based on the general phase equilibria Eq. (7.11), the criterion for azeotrope formation is:

$$K_j = \frac{y_j}{x_j} = \frac{\gamma_j^L f_j^L}{\bar{\phi}_j^V P} = 1 \qquad j = 1, \ldots, C \tag{7.15}$$

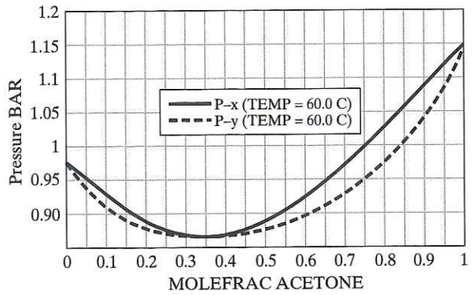

(a)

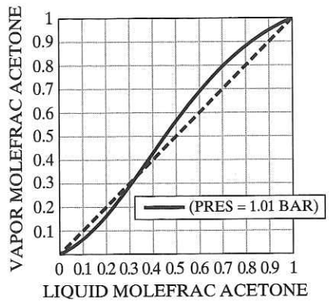

(b)

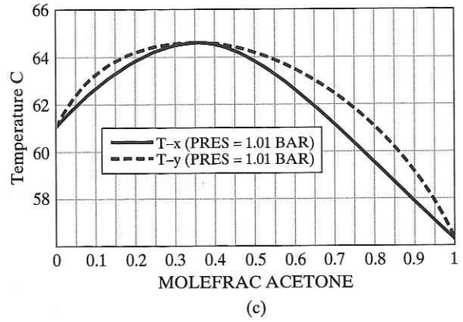

(c)

Figure 7.20 Phase diagrams for the acetone–chloroform binary computed using ASPEN PLUS: (a) *P–x–y* diagram at 60°C; (b) *x–y* diagram at 101 kPa; (c) *T–x–y* diagram at 101 kPa.

where the degree of nonideality is expressed by the deviations from unity of the activity coefficients and fugacities for the liquid phase and the fugacity coefficients for the vapor phase. At low pressure, $\bar{\phi}_j^V = 1$ and $f_j^L = P_j^s$ so that Eq. (7.15) reduces to

$$K_j = \frac{y_j}{x_j} = \gamma_j^L \frac{P_j^s}{P} = 1 \qquad j = 1, \ldots, C \tag{7.16}$$

Because the *K*-values for all of the species are unity at an azeotrope point, a simple distillation approaches this point, at which no further separation can occur. For this reason, an azeotrope is often called a *stationary* or *fixed* or *pinch point*.

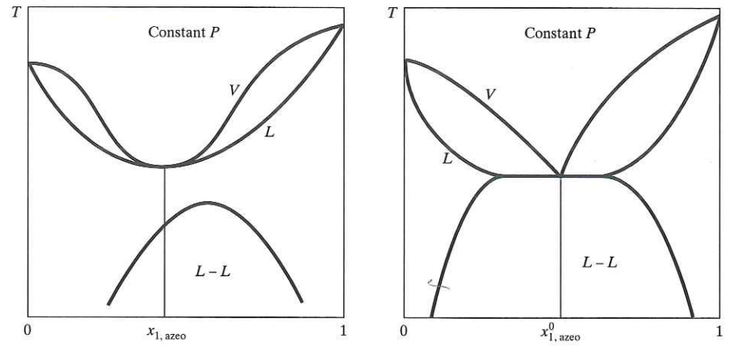

Figure 7.21 Binary phase diagram at a fixed pressure for: (a) homogeneous azeotrope; (b) heterogeneous azeotrope.

For a minimum-boiling azeotrope, when the deviations from Raoult's law are sufficiently large ($\gamma_j^L \gg 1.0$, usually > 7), splitting of the liquid phase into two liquid phases (phase splitting) may occur and a minimum-boiling, heterogeneous azeotrope may form that has a vapor phase in equilibrium with the two liquid phases. A heterogeneous azeotrope occurs when the vapor–liquid envelope overlaps with the liquid–liquid envelope, as illustrated in Figure 7.21b. For a homogeneous azeotrope, when $x_1 = x_{1,\text{azeo}} = y_1$, the mixture boils at this composition, as shown in Figure 7.21a; whereas for a heterogeneous azeotrope, when the overall liquid composition of the two liquid phases, $x_1 = x^0_{1,\text{azeo}} = y_1$, the mixture boils at this overall composition, as illustrated in Figure 7.21b, but the three coexisting phases have distinct compositions.

Residue Curves

To understand better the properties of azeotropic mixtures that contain three chemical species, it helps to examine the properties of *residue curves* on a ternary diagram. A collection of residue curves, which is called a *residue curve map*, can be computed and drawn by any of the major simulation programs. Each residue curve is constructed by tracing the composition of the equilibrium liquid residue of a simple (Rayleigh batch) distillation in time, starting from a selected initial composition of the charge to the still, using the following numerical procedure.

Consider L moles of liquid with mole fractions x_j ($j = 1, \ldots, C$), in a simple distillation still at its bubble point, as illustrated in Figure 7.22. Note that the still contains no trays and

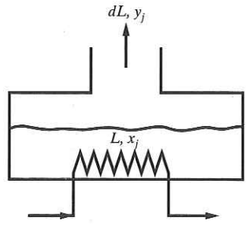

Figure 7.22 Simple distillation still.

no reflux is provided. As heating begins, a small portion of this liquid, ΔL moles, is vaporized. The instantaneous vapor phase has mole fractions y_j ($j = 1, \ldots, C$), assumed to be in equilibrium with the remaining liquid. Since the residual liquid, $L - \Delta L$ moles, has mole fractions $x_j + \Delta x_j$, the mass balance for species j is given by

$$Lx_j = (\Delta L)y_j + (L - \Delta L)(x_j + \Delta x_j) \qquad j = 1, \ldots, C-1 \tag{7.17}$$

In the limit, as $\Delta L \to 0$,

$$\frac{dx_j}{dL/L} = x_j - y_j = x_j\,(1 - K_j\,[T, P, \underline{x}, \underline{y}]) \qquad j = 1, \ldots, C-1 \tag{7.18}$$

and setting, $d\hat{t} = dL/L$,

$$\frac{dx_j}{d\hat{t}} = x_j - y_j \qquad j = 1, \ldots, C-1 \tag{7.19}$$

where K_j is given by Eq. (7.15). In Eq. (7.19), $\hat{t}$ can be interpreted as the dimensionless time, with the solution defining a family of residue curves, as illustrated in Figure 7.23. Note that each residue curve is the locus of the compositions of the residual liquid in time, as vapor is boiled off from a simple distillation still. Often, an arrow is assigned in the direction of increasing time (and increasing temperature). Note that the residue curve map does not show the equilibrium vapor composition corresponding to each point on a residue curve.

Yet another important property is that the *fixed points* of the residue curves are points where the driving force for a change in the liquid composition is zero; that is, $d\underline{x}/d\hat{t} = 0$. This condition is satisfied at the azeotropic points and the pure species vertices. For a ternary mixture with a single binary azeotrope, as in Figure 7.23, there are four fixed points on the triangular diagram: the binary azeotrope and the three vertices. Furthermore, the behavior of the residue curves in the vicinity of the fixed points depends on their stability. When all of the residue curves are directed by the arrows to the fixed point, it is referred to as a *stable node*, as illustrated in Figure 7.24a; when all are directed away, the fixed point is an *unstable node* (as in Figure 7.24b); and finally, when some of the residue curves are directed to and others are directed away from the fixed point, it is referred to as a *saddle point* (as in Figure 7.24c). Note that for a ternary system, the stability can be determined by calculating the eigenvalues of the Jacobian matrix of the nonlinear ordinary differential equations that comprise Eq. (7.19).

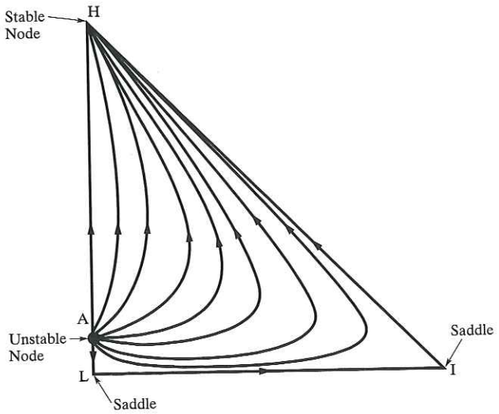

Figure 7.23 Residue curves of a ternary system with a minimum-boiling binary azeotrope.

Figure 7.24 Stability of residue curves for a ternary system in the vicinity of a binary azeotrope.

As an example, consider the residue curve map for a ternary system with a minimum-boiling binary azeotrope of heavy (H) and light (L) species, as shown in Figure 7.23. There are four fixed points: one unstable node at the binary azeotrope (A), one stable node at the vertex for the heavy species (H), and two saddles at the vertices of the light (L) and intermediate (I) species.

It is of special note that the boiling points and the compositions of all azeotropes can be used to characterize residue curve maps. In fact, even without a simulation program to compute and draw the detailed diagrams, this information alone is sufficient to sketch the key characteristics of these diagrams using the following procedure. First, the boiling points of the pure species are entered at the vertices. Then the boiling points of the binary azeotropes are positioned at the azeotropic compositions along the edges, with the boiling points of any ternary azeotropes positioned at their compositions within the triangle. Arrows are assigned in the direction of increasing temperature in a simple distillation still. As examples, typical diagrams for mixtures involving binary and ternary azeotropes are illustrated in Figure 7.25. Figure 7.25a is for a simple system, without azeotropes, involving nitrogen, oxygen, and

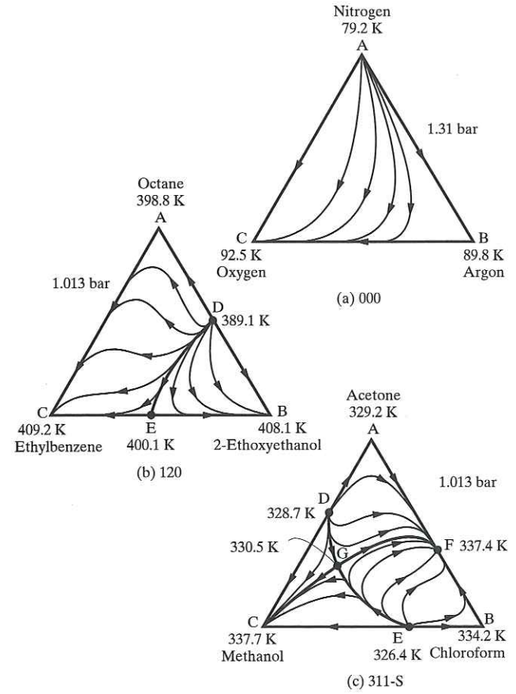

Figure 7.25 Maps of residue curves or distillation lines: (a) system without azeotropes; (b) system with two binary azeotropes; (c) system with binary and ternary azeotropes (Stichlmair et al., 1989).

argon. In this mixture, nitrogen is the lowest-boiling species (L), argon is the intermediate boiler (I), and oxygen is the highest-boiling species (H). Thus, along the oxygen–argon edge the arrow is pointing to the oxygen vertex, and on the remaining edges the arrows point away from the nitrogen vertex. Since these arrows point away at the nitrogen vertex, it is an unstable node, and all of the residue curves emanate from it. At the argon vertex, the arrows point to and away from it. Since the residue curves turn in the vicinity of this vertex, it is not a terminal point. Rather, it is referred to as a saddle point. All of the curves end at the oxygen vertex, which is a terminal point or stable node. For this ternary mixture, the map shows that pure argon, the intermediate boiler, cannot be obtained in a simple distillation.

Simple Distillation Boundaries

The graphical approach described here is effective in locating the starting and terminal points and the qualitative locations of the residue curves. As illustrated in Figures 7.25b and 7.25c, it works well for binary and ternary azeotropes that exhibit multiple starting and terminal points. In these cases, one or more *simple distillation boundaries* called *separatrices* (e.g., curved line DE in Figure 7.25b) divide these diagrams into regions with distinct pairs of starting and terminal points. For the separation of homogeneous mixtures by simple distillation, these separatrices cannot be crossed unless they are highly curved. A feed located in region ADECA in Figure 7.25b has a starting point approaching the composition of the binary azeotrope of octane and 2-ethoxyethanol and a terminal point approaching pure ethylbenzene, whereas a feed located in region DBED has a starting point approaching the same binary azeotrope but a terminal point approaching pure 2-ethoxyethanol. In this case, a pure octane product is not possible. Figure 7.25c is even more complex. It shows four distillation boundaries (curved lines GC, DG, GF, and EG), which divide the diagram into four distillation regions.

Distillation Towers

When tray towers are modeled assuming vapor–liquid equilibrium at each tray, the residue curves approximate the liquid composition profiles at *total reflux*. To show this, a species balance is performed for the top n trays, counting down the tower, as shown in Figure 7.26:

$$L_{n-1}\underline{x}_{n-1} + D\underline{x}_D = V_n\underline{y}_n \tag{7.20}$$

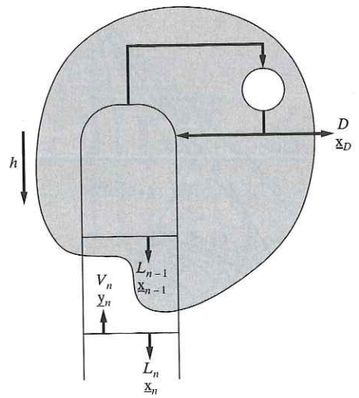

Figure 7.26 Schematic of rectifying section.

where D and $\underline{x}_D$ are the molar flow rate and vector of mole fractions of the distillate. Similarly, L_{n-1} and $\underline{x}_{n-1}$ are for the liquid leaving tray $n-1$, and V_n and $\underline{y}_n$ are for the vapor leaving tray n. Defining h as the dimensionless distance from the top of the tower, a backward-difference approximation at tray $n+1$ is

$$\left.\frac{d\underline{x}}{dh}\right|_{n+1} \cong \underline{x}_n - \underline{x}_{n-1} \tag{7.21}$$

Rearranging Eq. (7.20) and substituting in Eq. (7.21),

$$\left.\frac{d\underline{x}}{dh}\right|_{n+1} \cong \underline{x}_n - \frac{V_n}{L_{n-1}}\underline{y}_n + \frac{D}{L_{n-1}}\underline{y}_D \tag{7.22}$$

At total reflux, with $D = 0$ and $V_n = L_{n-1}$, Eq. (7.22) becomes

$$\left.\frac{d\underline{x}}{dh}\right|_{n+1} \cong \underline{x}_n - \underline{y}_n \tag{7.23}$$

Hence, Eq. (7.23) approximates the operating lines at total reflux and, because $\hat{t}$ and h are dimensionless variables and Eq. (7.19) is identical in form, the residue curves approximate the operating lines of a distillation tower operating at total reflux.

Distillation Lines

An exact representation of the operating line for a distillation tower at total reflux, also known as a *distillation line* [as defined by Zharov (1968) and Zharov and Serafimov (1975)], is shown in Figure 7.27. Note that, at total reflux,

$$\underline{x}_n = \underline{y}_{n+1} \qquad n = 0, 1, \ldots \tag{7.24}$$

Furthermore, assuming operation in vapor–liquid equilibrium, the mole fractions on tray n, $\underline{x}_n$, and $\underline{y}_n$ lie at the ends of the equilibrium tie lines.

To appreciate better the differences between distillation lines and residue curves, consider the following observations. First, Eq. (7.19) requires the tie line vectors connecting liquid composition $\underline{x}$ and vapor composition $\underline{y}$, at equilibrium, to be tangent to the residue curves, as illustrated in Figure 7.28. Since these tie line vectors must also be chords of the distillation lines, the residue curves and the distillation lines must intersect at the liquid composition $\underline{x}$. Note that when the residue curve is linear (as for binary mixtures), the tie lines and the residue curve are collinear, and consequently, the distillation lines coincide with the residue curves.

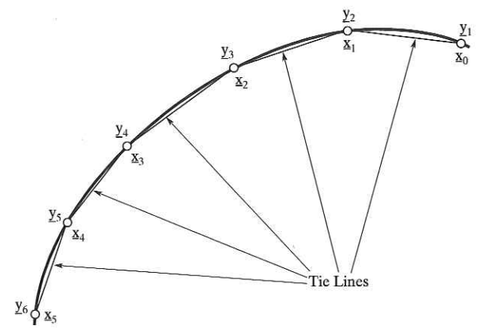

Figure 7.27 Distillation line and its tie lines.

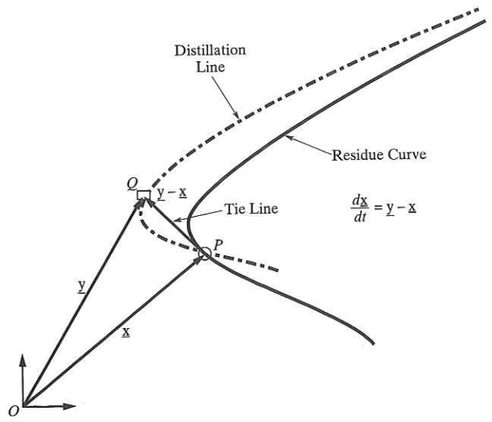

Figure 7.28 Residue curve and distillation line through *P*.

Figure 7.29a shows two distillation lines (δ_1 and δ_2) that intersect a residue curve at points A and B. As a consequence of Eq. (7.19), their corresponding vapor compositions at equilibrium, a and b, lie at the intersection of the tangents to the residue curves at A and B with the distillation lines δ_1 and δ_2. Clearly, the distillation lines do not coincide with the residue curves, an assumption that is commonly made but that may produce significant errors. In Figure 7.29b, a single distillation line connects the compositions on four adjacent trays (at C, D, E, F) and crosses four residue curves (ρ_C, ρ_D, ρ_E, ρ_F) at these points.

Note that distillation lines are generated by computer as easily as residue curves and, because they do not involve any approximations to the operating line at total reflux, are preferred for the analyses to be performed in the remainder of this section. However, simulation programs compute and plot only residue curves. It can be shown that distillation lines have the same properties as residue curves at fixed points, and hence, both families of curves are sketched similarly. Their differences are pronounced in regions that exhibit extensive curvature.

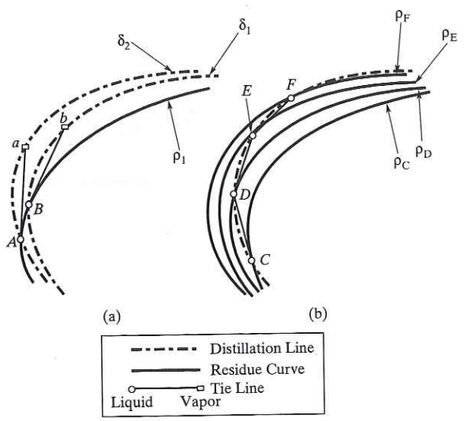

Figure 7.29 Geometric relationship between distillation lines and residue curves.

Computing Azeotropes for Multicomponent Mixtures

Gmehling (1994) provides data on more than 15,000 binary azeotropes and 900 ternary azeotropes. Undoubtedly, many more ternary azeotropes exist, as well as untold numbers of azeotropes involving more than three components. When a process simulation program is used to compute a residue curve map for a ternary system at a specified pressure, compositions and temperatures of all azeotropes are automatically estimated. The results depend, of course, on the selected vapor pressure and liquid-phase activity coefficient correlations. For quaternary and higher systems, the arclength homotopy-continuation method of Fidkowski, Malone, and Doherty (1993) can be used for homogeneous systems to estimate all azeotropes. They find all roots to the following equations, which define a homogeneous azeotrope:

$$y_j - x_j = 0, \qquad j = 1, 2, \ldots, C-1 \tag{7.25}$$

$$y_j = \left(\frac{\gamma_j^L P_j^s}{\bar{\phi}_j^V P}\right) x_j, \qquad j = 1, 2, \ldots, C \tag{7.26}$$

$$\sum_{j=1}^{C} x_j = 1 \tag{7.27}$$

$$\sum_{j=1}^{C} y_j = 1 \tag{7.28}$$

$$x_j \geq 0, \qquad j = 1, 2, \ldots, C \tag{7.29}$$

To find the roots, they construct the following homotopy to replace Eqs. (7.25) and (7.26), based on gradually moving from an ideal *K*-value based on Raoult's law to the more rigorous expression of Eq. (7.26):

$$y_j - x_j = \left[(1-t) + t\frac{\gamma_j^L}{\bar{\phi}_j^V}\right]\frac{P_j^s}{P} x_j = H(t, x_j) = 0, \qquad j = 1, 2, \ldots, C \tag{7.30}$$

Initially, the homotopy parameter, t, is set to 0 and all values of x_j are set to 0 except for one, which is set to 1.0. Then t is gradually and systematically increased until a value of 1.0 is obtained. With each increase, the temperature and mole fractions are computed. If the resulting composition at $t = 1.0$ is not a pure component, it is an azeotrope. By starting from each pure component, all azeotropes are computed. The method of Fidkowski, Malone, and Doherty is included in many of the process simulation programs. Eckert and Kubicek (1997) extended the method of Fidkowski, Malone, and Doherty to the estimation of heterogeneous multicomponent azeotropes.

Distillation-Line Boundaries and Feasible Product Compositions

Of great practical interest is the effect of distillation boundaries on the operation of distillation towers. To summarize a growing body of literature, it is well established that the compositions of a distillation tower operating at total reflux cannot cross the distillation-line boundaries, except under unusual circumstances, where these boundaries exhibit a high degree of curvature. This provides the total-reflux bound on the possible (feasible) compositions for the distillate and bottoms products.

As shown in Figure 7.30a, at total reflux, $\underline{x}_B$ and $\underline{y}_D$ reside on a distillation line. Furthermore, these compositions lie collinear with the feed composition, $\underline{x}_F$, on the overall material balance line. As the number of stages increases, the operating curve becomes more convex and in the limit approaches the two sides of the triangle that meet at the intermediate boiler. As an example, an operating line at total reflux (minimum stages) is the curve AFC in Figure 7.31a. At the other extreme, as the number of stages increases, the operating curve becomes more convex approaching ABC, where the number of stages approaches infinity (corresponding to minimum

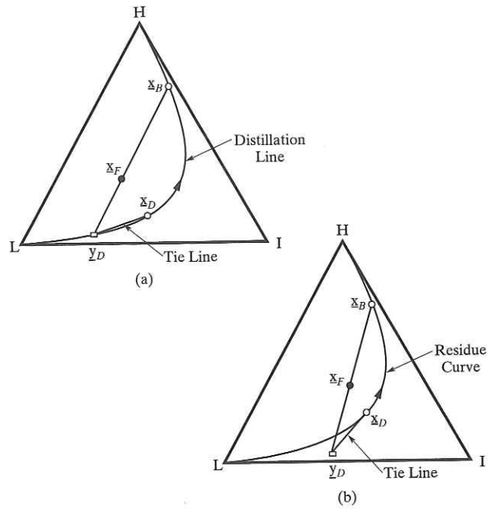

Figure 7.30 Overall mass balance line with a partial/total condenser.

reflux). Hence, the operating line for a distillation tower that operates within these limiting regimes lies within the region ABCFA in Figure 7.31a. Note that when a distillation tower operates with a partial condenser, as the feed and product streams are decreased toward total reflux, the last bubble of vapor distillate has the mole fractions, $\underline{y}_D$, as shown in Figures 7.30a and 7.30b. Consequently, as total reflux is approached, the material balance line connecting the bottoms, feed, and distillate mole fractions is shown. Figure 7.30a shows the distillation line that passes through the $\underline{x}_B$ and $\underline{y}_D$ mole fractions, while Figure 7.30b shows the residue curve that passes through the $\underline{x}_D$ mole fractions, and approximately through the $\underline{x}_B$ mole fractions.

Two additional bounds in Figure 7.31a are obtained as follows. First, in the limit of a pure nitrogen distillate, the line AFE represents a limiting overall material balance for a feed composition at point F, with point E at the minimum concentration of oxygen in the bottoms product. Similarly, in the limit of a pure oxygen bottoms, the line CFD represents a limiting overall material balance, with point D at the minimum concentration of nitrogen in the distillate along the nitrogen–argon axis. Hence, the distillate composition is confined to the shaded region ADFA, and the bottoms product composition lies in the shaded region, CEFC. Operating lines that lie within the region ABCFA connect the distillate and bottoms product compositions in these shaded regions. At best, only one pure species can be obtained. In addition, only those species located at the end points of the distillation lines can be recovered in high purity, with one exception to be noted. Hence, the end points of the distillation lines determine the potential distillate and bottoms products for a given feed. This also applies to the complex mixtures in Figures 7.31b and 7.31c. Here, the location of the feed point determines the *distillation region* in which the potential distillate and bottoms product compositions lie. For example, in Figure 7.31b, for feed F, only pure 2-ethoxyethanol can be obtained. When the feed is moved to the left across the distillation-line boundary, pure ethylbenzene can be obtained. In Figure 7.31c, only methanol can be recovered in high purity for feeds in the region LTGCL. For a feed in the region EDTHGBE, no pure product is possible. Before attempting rigorous distillation calculations with a simulation program, it is essential to establish, with the aid of computer-generated residual curve maps, regions of product-composition feasibility such as shown in Figure 7.31. Otherwise it is possible to waste much time and effort in trying to converge distillation calculations when specified product compositions are impossible.

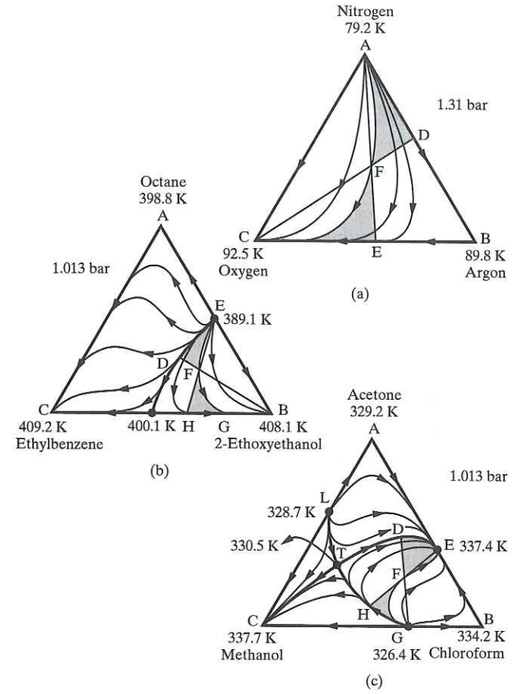

Figure 7.31 Regions of feasible distillate and bottoms product compositions (shaded) for a ternary mixture: (a) system without azeotropes; (b) system with two binary azeotropes; (c) system with binary and ternary azeotropes (Stichlmair et al., 1989).

Heterogeneous Distillation

In heterogeneous azeotropic distillation, an entrainer is utilized that concentrates in the overhead vapor and, when condensed, causes the formation of a second liquid phase that can be decanted and recirculated to the tower as reflux. The other liquid phase as well as the bottoms are the products from the distillation. This is possible when the entrainer forms a heterogeneous azeotrope with one or more of the species in the feed. Figure 7.32a shows one possible configuration, with an accompanying triangular diagram in Figure 7.32b for the dehydration of ethanol using toluene as an entrainer. In Column C-1, the feed is preconcentrated in ethanol. Column C-2 is the azeotropic tower. Unfortunately, both products, B1 and B2 are bottoms. Ethanol and water form a minimum-boiling azeotrope at 89 mol% ethanol and 1 atm, as shown in Figures 7.32c and 7.32d, which were prepared by ASPEN PLUS. Although toluene is the highest-boiling species, it is an appropriate entrainer because it forms minimum-boiling azeotropes with both water and ethanol. Hence, the arrows on the residue curves point toward both the ethanol and water vertices, allowing ethanol to be recovered in a high-purity bottoms product. Since toluene forms a ternary, minimum-boiling, heterogeneous azeotrope (point D2 in Figure 7.32b), the overhead vapor approaches this composition and condenses into two liquid phases, one rich in toluene (point S2 in Figure 7.32b) and the other rich in water (point S1 in Figure 7.32b), which are separated in the decanter. The former is recycled to the azeotropic tower, while the latter is recycled to the preconcentrator. All column product compositions are shown in Figure 7.32b. A binodal curve for the distillate temperature of the azeotropic tower is included in Figure 7.32b together with a tie line through the azeotropic composition of D2 to show the phase split of condensed overhead D2 into liquid phases S1 and S2.

When residue curve and distillation-line maps are constructed for heterogeneous systems, using process simulation programs, the composition spaces are also divided into regions with simple distillation boundaries. However, the residue curve and distillation-line maps for systems containing heterogeneous azeotropes are far more restricted. Their azeotropic points can only be minimum-boiling saddles or unstable nodes. More importantly, the compositions of the two liquid phases lie within different distillation regions. This unique property, which is not shared by homogeneous systems, enables the decanter to bridge the distillation regions. This is the key that permits the compositions of a single distillation column to cross from one distillation region into another, as illustrated in Figures 7.32a and 7.32b. In this system, for the dehydration of ethanol using toluene, the preconcentrator, C-1 with mixed feed, M1, removes water, B1, as the bottoms product. Its distillate, at D1, lies just to the right of the simple distillation boundary, K(D2)L, as shown in Figure 7.32b. The addition of entrainer, S2, to the distillate, D1, produces a C-2 feed stream, M2, that crosses this boundary into the distillation region just to the left of boundary K(D2) where high-purity ethanol, B2,

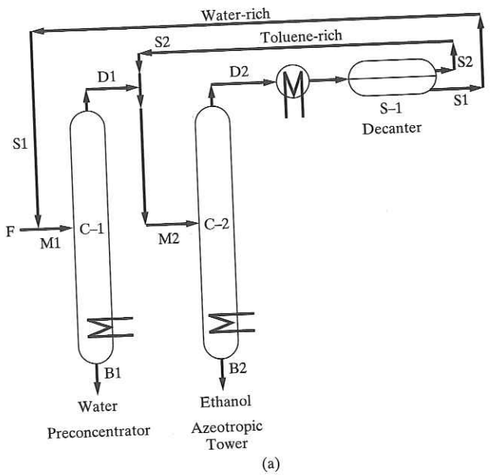

(a)

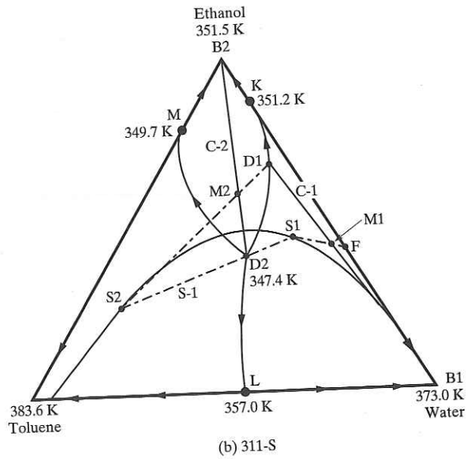

(b) 311-S

Figure 7.32 Dehydration of ethanol using toluene as an entrainer: (a) process flow diagram; (b) ternary composition diagram; (c) *T–x–y* diagram at 1 atm; (d) *x–y* diagram at 1 atm (Stichlmair et al., 1989).

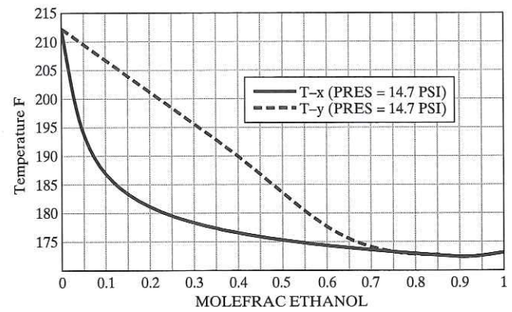

(c)

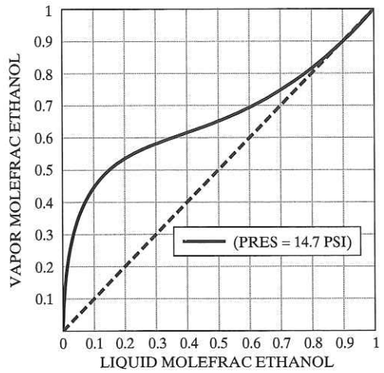

(d)

Figure 7.32 (*Continued*)

is obtained as the bottoms product of the azeotropic tower, C-2. Its overhead vapor, D2, is in the vicinity of the heterogeneous ternary azeotrope, and when condensed and subcooled forms two liquid phases that are decanted easily. The organic phase, at S2, lies in a different distillation region than the feed, M1, to column C-1. When combined with D1, the feed, M2, is on the other side of the simple distillation boundary, in the region M(D2)K(B2)M. The toluene-rich phase, S2, is recycled to column C-2, and the water-rich phase, S1, is combined with the fresh feed (F) to column C-1. The distillate and bottoms products of both towers and their overall mass balance lines are shown in Figure 7.32b.

The distillation sequence shown in Figure 7.32a is only one of several sequences, involving from two to four columns, that have been proposed and/or applied in industry for separating a mixture by employing heterogeneous azeotropic distillation. Most common is the three-column sequence from the study of Ryan and Doherty (1989), as shown in Figure 7.33a. When used to separate a mixture of ethanol and water using benzene as the entrainer, the three columns perform the separation in the following manner, where the material-balance lines for Columns 2 and 3 are shown in Figure 7.33b. The aqueous feed, F1, dilute in ethanol, is preconcentrated in Column 1 to obtain a pure water bottoms, B1, and a distillate, D1, whose composition approaches that of the homogeneous minimum-boiling binary azeotrope. The distillate becomes the feed to Column 2, the azeotropic column, where nearly pure ethanol, B2, is removed as bottoms. The overhead vapor from Column 2, V2, is close to the composition of the heterogeneous ternary azeotrope of ethanol, water, and benzene. When condensed, it separates into two liquid phases in the decanter. Most of the organic-rich phase, L2, is returned to

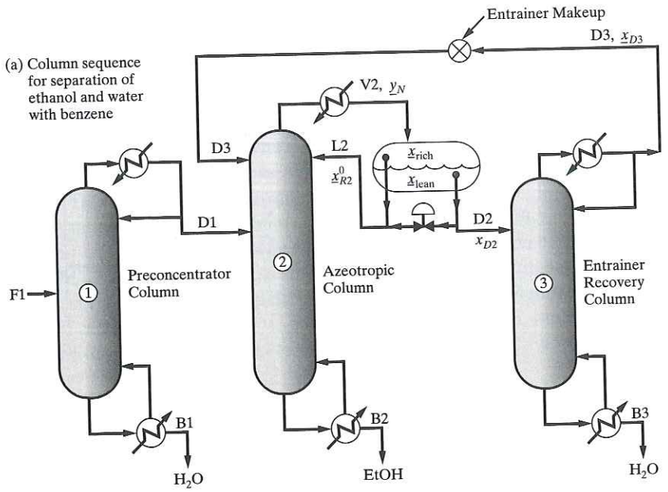

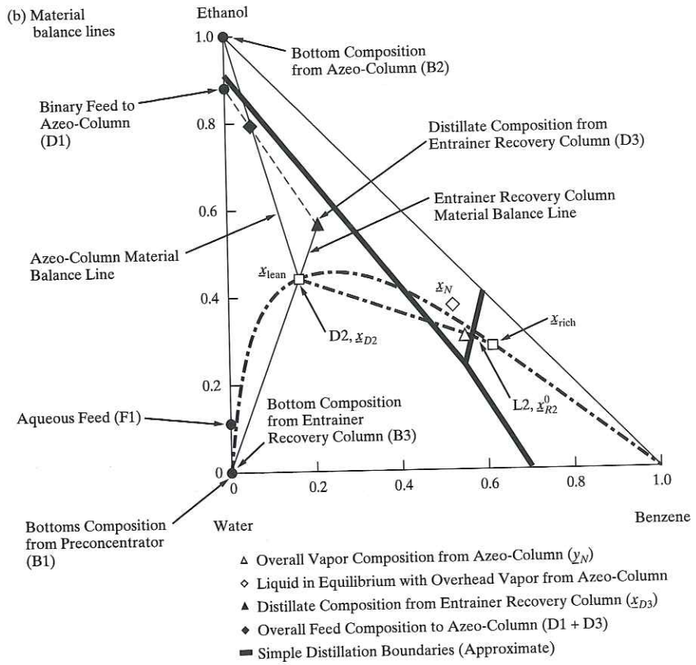

Figure 7.33 Kubierschky three-column system.

Column 2 as reflux. Most of the water-rich phase, D2, is sent to Column 3, the entrainer recovery column. Here, the distillate, D3, consisting mainly of ethanol, but with appreciable amounts of benzene and water, is recycled to the top of Column 2. The bottoms, B3, from Column 3 is nearly pure water. All columns operate at close to 1 atm pressure.

Multiple Steady States

The occurrence of multiple steady states in chemical reactors has been well recognized for at least 50 years. The most common example is an adiabatic CSTR, for which in some cases, for the same feed and reactor size, three possible products may be obtained, two of which are stable and one unstable, as shown in Case Study 21.1. The product obtained in actual operation depends upon the startup procedure for the reactor. Only in the last 25 years has the existence of multiple steady states in distillation towers been shown by calculations and verified by experimental data from tower operation. In particular, azeotropic distillation is particularly susceptible to multiple steady states. Disturbances during operation of an azeotropic tower can cause it to switch from one steady state to another as shown by Prokopakis and Seider (1983). Methods for computing multiple steady states for homogeneous and heterogeneous azeotropic distillation are presented in a number of publications. Kovach and Seider (1987) computed, by an arclength homotopy-continuation method, five steady states for the ethanol–benzene–water distillation. Bekiaris et al. (1993, 1996, 2000) studied multiple steady states for ternary homogeneous- and ternary heterogeneous-azeotropic distillation, respectively. Using the distillate flow rate as the bifurcation parameter, they found conditions of feed compositions and distillation-region boundaries for which multiple steady states can occur in columns operating at total reflux (infinite reflux ratio) with an infinite number of equilibrium stages (referred to as the ∞–∞ case). They showed that their results have relevant implications for columns operating at finite reflux ratios with a finite number of stages. Vadapalli and Seader (2001) used ASPEN PLUS with an arclength continuation and bifurcation method to compute all stable and unstable steady states for azeotropic distillation under conditions of finite reflux ratio and finite number of equilibrium stages. Specifications for their heterogeneous azeotropic distillation example, involving the separation of an ethanol–water mixture using benzene, are shown in Figure 7.34a. The total feed rate to the column is 101.962 kmol/hr. The desired bottoms product is pure ethanol. Using the bottoms flow rate, as the bifurcation parameter, computed results for the mole fraction of ethanol in the bottoms are shown in Figure 7.34b as a function of the bifurcation parameter. In the range of bottoms flow rate from approximately 78 to 96 kmol/hr, three steady states exist, two stable and one unstable. For a bottoms rate equal to the flow rate of ethanol in the feed (89 kmol/hr), the best stable solution is an ethanol mole fraction of 0.98; the inferior stable solution is only 0.89. Figure 7.34b shows the computed points. In the continuation method, the results of one point are used as the initial guess for obtaining an adjacent point.

While heterogeneous azeotropic distillation towers are probably used more widely than their homogeneous counterparts, care must be taken in their design and operation. In addition to the possibility of multiple steady states, most azeotropic distillation towers involve sharp fronts as the temperatures and compositions shift abruptly from the vicinity of one fixed point to the vicinity of another. Furthermore, in heterogeneous distillations, sharp fronts often accompany the interface between trays having one and two liquid phases as well. Consequently, designers must select carefully the number of trays and the reflux rates to prevent these fronts from exiting the tower with an associated deterioration in the product quality. While these and other special properties of azeotropic towers (e.g., maximum reflux rates above which the separation deteriorates, and an insensitivity of the product compositions to the number of trays) are complicating factors, fortunately, they are usually less important when synthesizing separation trains, and consequently they are not discussed further here. For a review of the literature on this subject, see the article by Widagdo and Seider (1996).